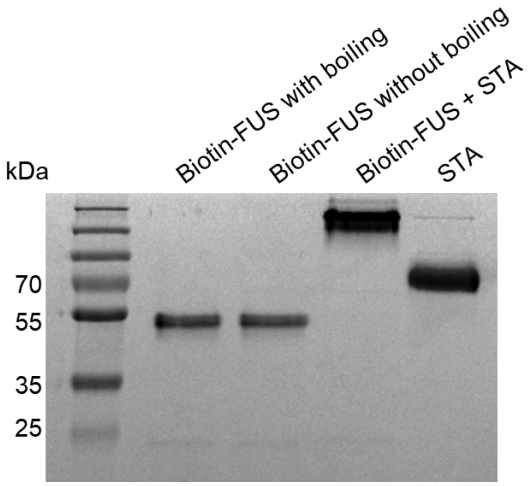

Figure S1. SDS-PAGE analysis of biotinylated FUS (Biotin-FUS) and its interaction with streptavidin (STA). STA-bound Biotin-FUS proteins remained clustered during SDS-PAGE without boiling.

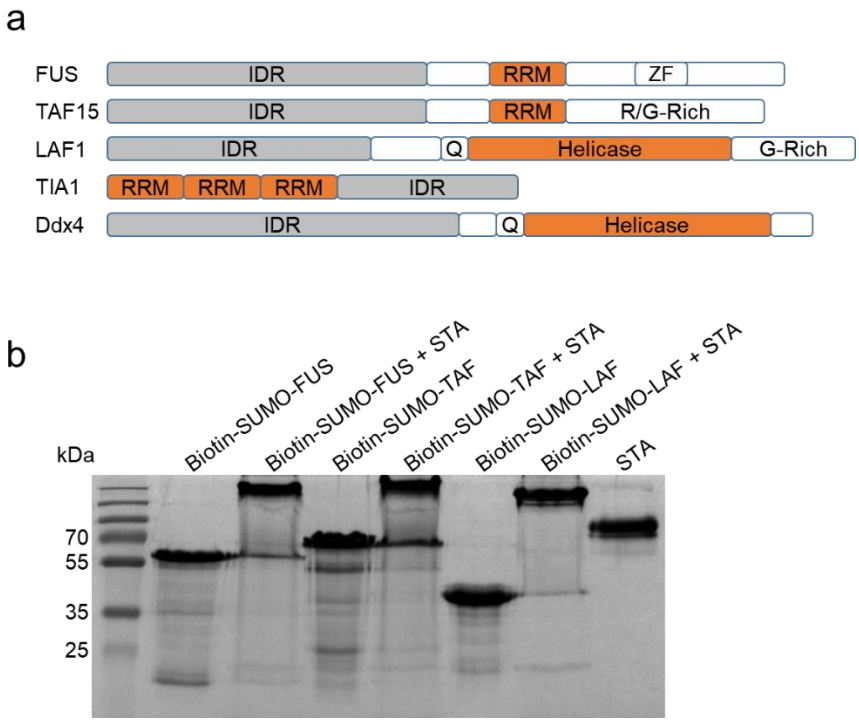

Figure S2. SUMO-fused IDR proteins. (**a)** Schematic diagrams of full-length IDPs that are investigated in the present study. All IDPs contain various functional domains with defined structures. **(b)** SDS-PAGE analysis of STA-induced clustering of biotin-SUMO-fused IDR proteins (FUS, TAF, and LAF).

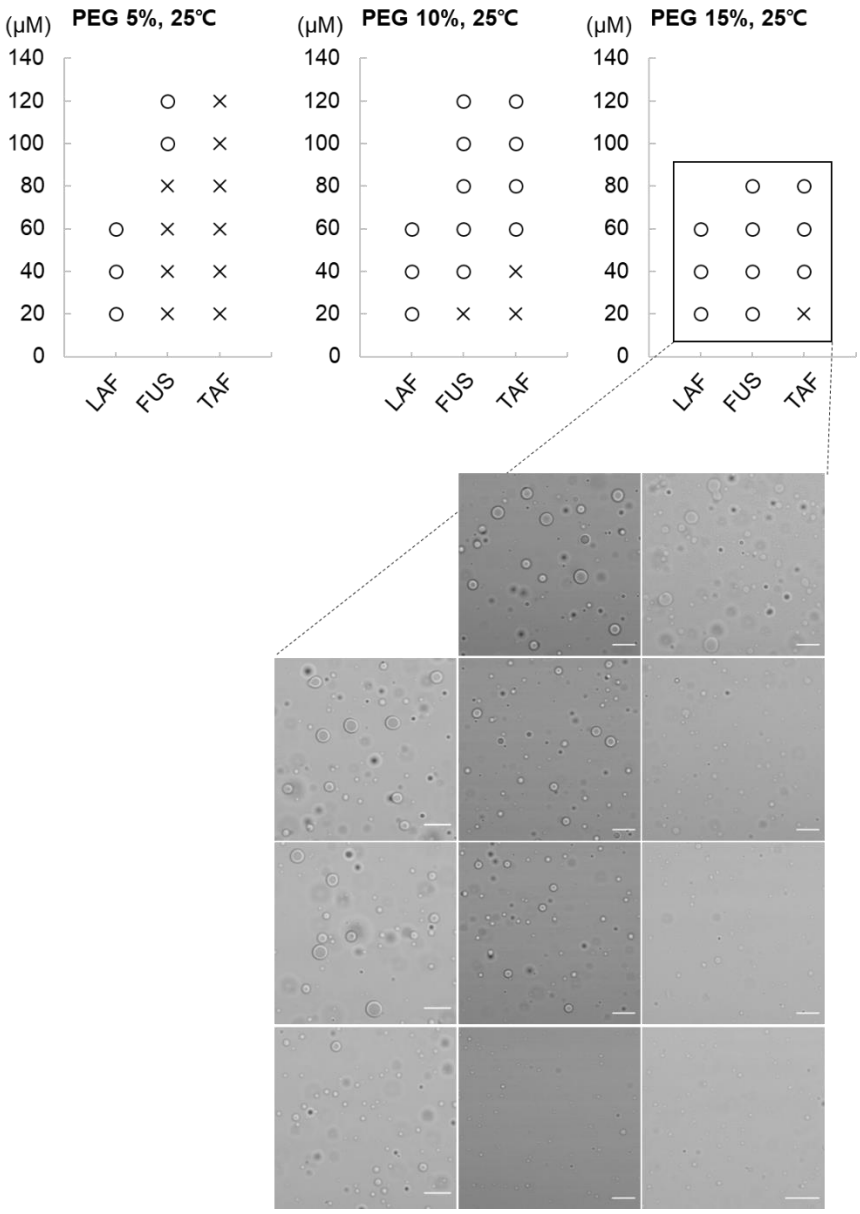

Figure S3. Phase diagrams of three biotin-SUMO fused IDRs at different PEG concentration. Circle dots indicate phase separation. Optical images of IDR droplets that are formed with 15% PEG are shown below. Scale bars 10 μm.

Note: Molecular crowding reagent PEG reduced threshold concentrations for IDR droplet generation. For various subsequent droplet analysis, 80 μM of FUS and TAF or 60 μM of LAF with 15% PEG was used for droplet generation. In this condition, droplets with diameters lager than 5 μm were readily formed, which is required for reliable FRAP measurements for protein diffusion inside droplets.

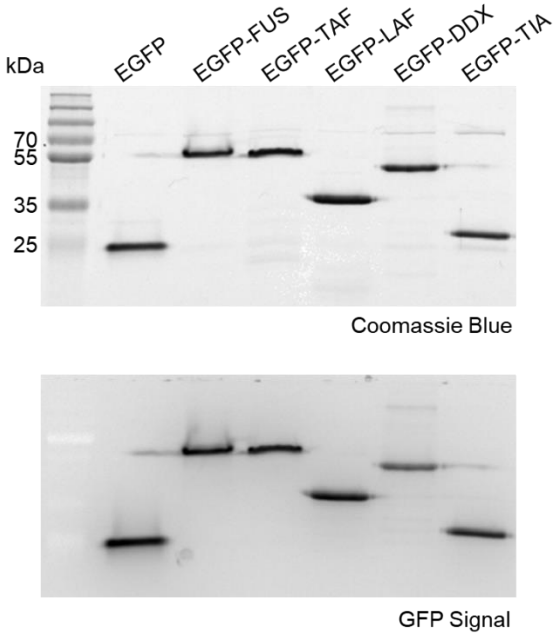

Figure S4. SDS-PAGE analysis of EGFP-fused IDR client proteins without boiling. An EGFR fluorescence image was also obtained (below).

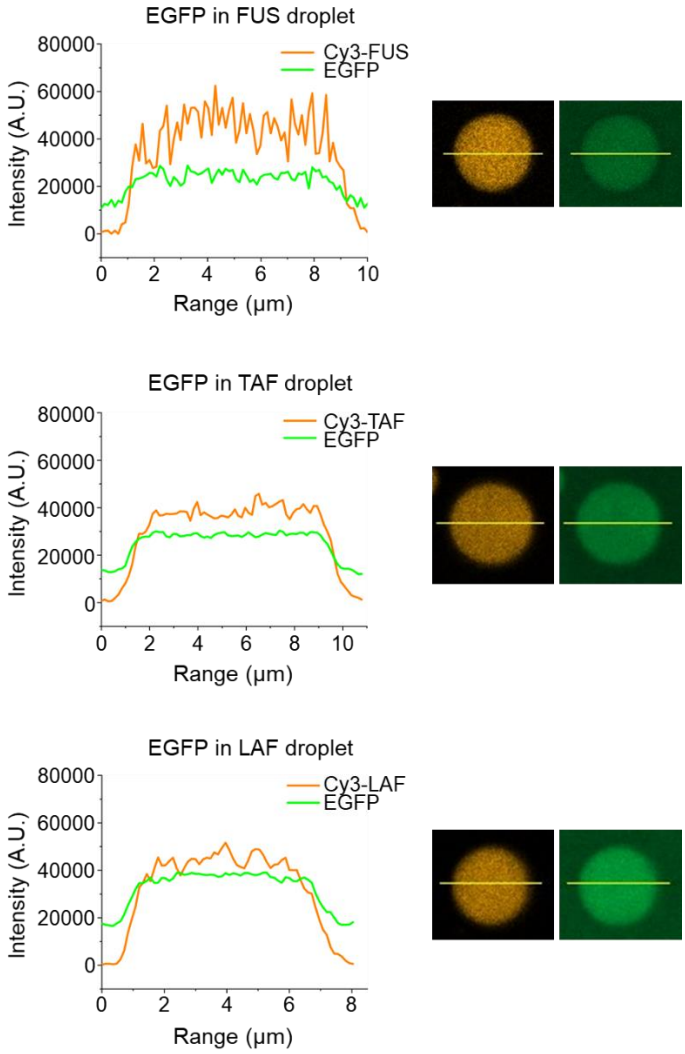

Figure S5. Fluorescence intensity diagrams and images of IDR droplets with free EGFP. Fluorescence intensities of free EGFP client (green) as well as three Cy3-labeled scaffold IDRs (orange) are shown. Droplets over 5 μm were selected for analysis.

Note: Diagrams indicate fairly uniform protein distribution inside droplets. While EGFP signals are clearly higher inside droplets, partition coefficients were less than 2 due to high background (outside droplet) signals.

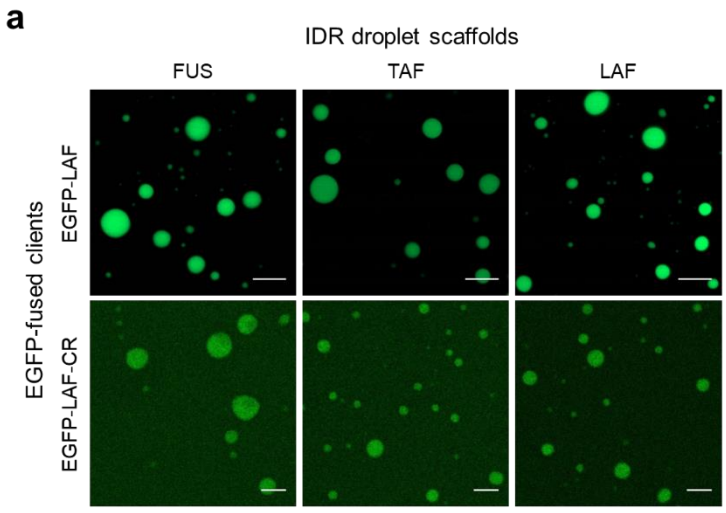

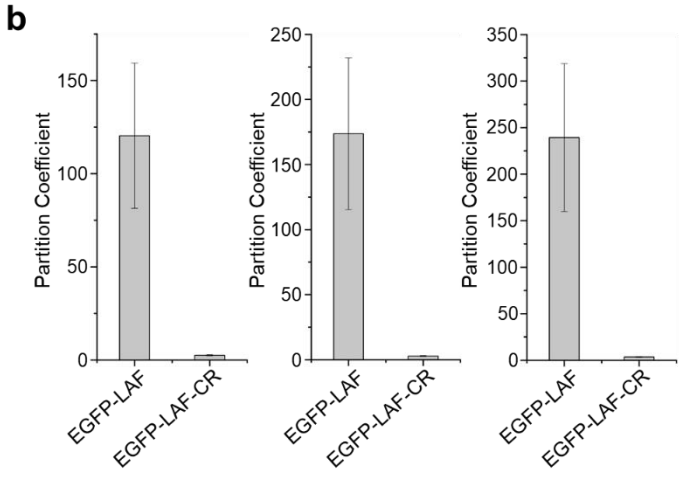

	EGFP-LAF	EGFP-LAF-CR
FUS	120.4 ± 39	2.5 ± 0.3
TAF	173.7 ± 58.3	2.8 ± 0.4
LAF	239.3 ± 79.5	3.5 ± 0.4

c

	Length (a.a.)	Polar (S, T, N, Q)	+ Charge (R, K)	- Charge (D, E)	Aromatic (F, Y, W)	S, Q	G
FUS	**213**	52.1%	0.5%	2.3%	12.7%	44.1%	24.9%
LAF	**168**	22.0%	14.3%	11.9%	7.1%	8.3%	35.1%
LAF-CR	**168**	41.7%	0%	1.8%	11.9%	28.0%	35.1%

Figure S6. Recruitment of charge-removed LAF (EGFP-LAF-CR) into IDR droplets. (a) Fluorescence images of three IDR droplets (FUS, TAF, LAF) with EGFP-LAF and EGFP-LAF-CR clients. Scale bar = 10 μm. **(b)** Partition coefficients (PCs) (inside/outside droplets) of client EGFP-LAF and EGFP-LAF-CR. Error bars: 1 s.d. (n = 100 from three independent experiments). **(c)** Amino acid compositions of FUS, LAF, and LAF-CR.

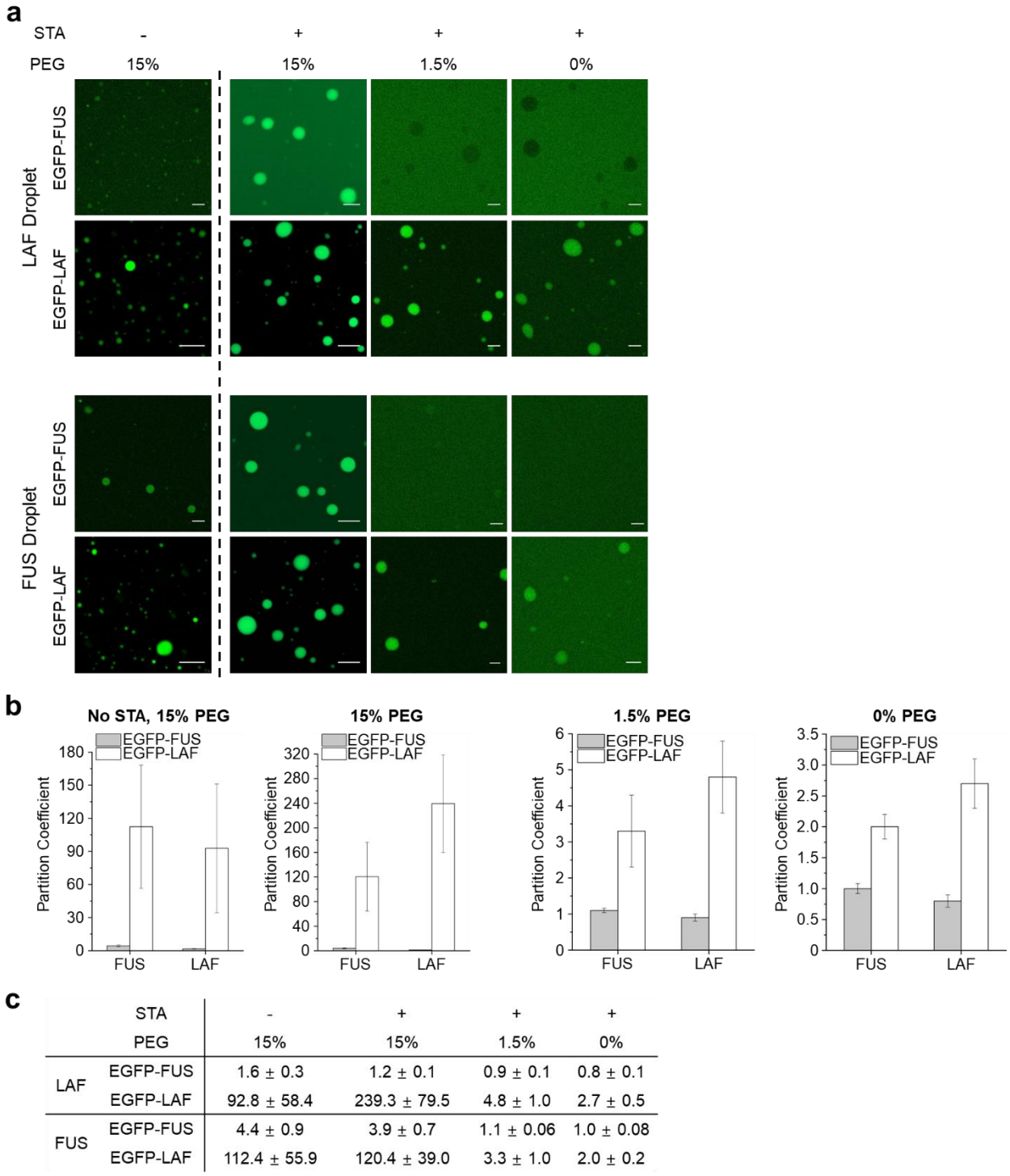

c

	STA	-	+	+	+
	PEG	15%	15%	1.5%	0%
LAF	EGFP-FUS	1.6 ± 0.3	1.2 ± 0.1	0.9 ± 0.1	0.8 ± 0.1
	EGFP-LAF	92.8 ± 58.4	239.3 ± 79.5	4.8 ± 1.0	2.7 ± 0.5
FUS	EGFP-FUS	4.4 ± 0.9	3.9 ± 0.7	1.1 ± 0.06	1.0 ± 0.08
	EGFP-LAF	112.4 ± 55.9	120.4 ± 39.0	3.3 ± 1.0	2.0 ± 0.2

Figure S7. Effects of STA clustering and a high crowding reagent concentration (15% PEG) in unusual LAF/FUS client recruitment. (a) Fluorescence images of EGFP-FUS and EGFP-LAF recruited into FUS and LAF droplets without STA or with varying PEG concentrations (15%, 1.5%, and 0%). Scale bar = 10 μm. **(b), (c)** Partition coefficients of recruited EGFP-FUS and EGFP-LAF into FUS and LAF droplets without STA or with varying PEG concentrations (15%, 1.5%, and 0%). Error bars: 1 s.d. (n = 100 from three independent experiments). 15% PEG data from Figure 2

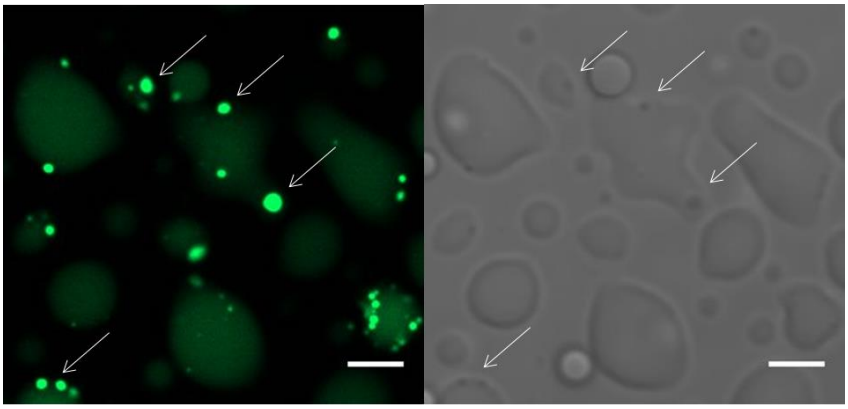

Figure S8. Subcompartments of client EGFP-DDX inside FUS droplets. Distinct EGFP-DDX client subcompartments (arrows) inside FUS droplets are clearly observed with fluorescence (left) and differential interference contrast (DIC, right) images. Scale bars 5 μm.

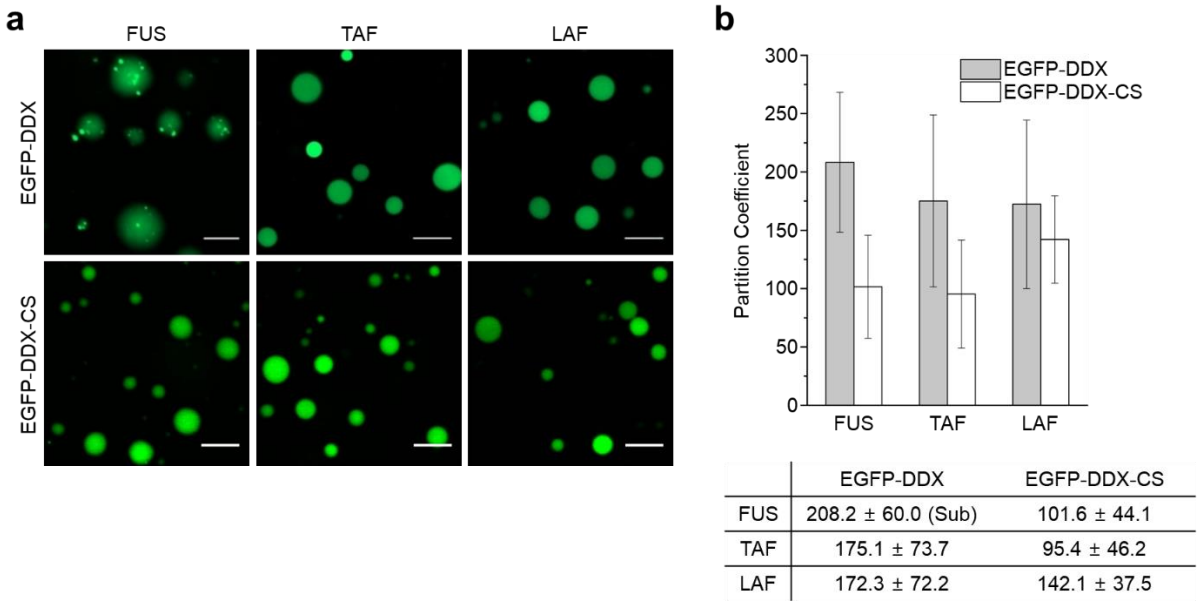

	EGFP-DDX	EGFP-DDX-CS
FUS	208.2 ± 60.0 (Sub)	101.6 ± 44.1
TAF	175.1 ± 73.7	95.4 ± 46.2
LAF	172.3 ± 72.2	142.1 ± 37.5

Figure S9. Recruitment of charge-scrambled DDX (EGFP-DDX-CS) into IDR droplets. (a) Fluorescence images of three IDR droplets (FUS, TAF, LAF) with EGFP-DDX and EGFP-DDX-CS clients. Scale bar = 10 μm. **(b)** Partition coefficients of client EGFP-DDX and EGFP-DDX-CS. Error bars: 1 s.d. (n = 100 from three independent experiments).

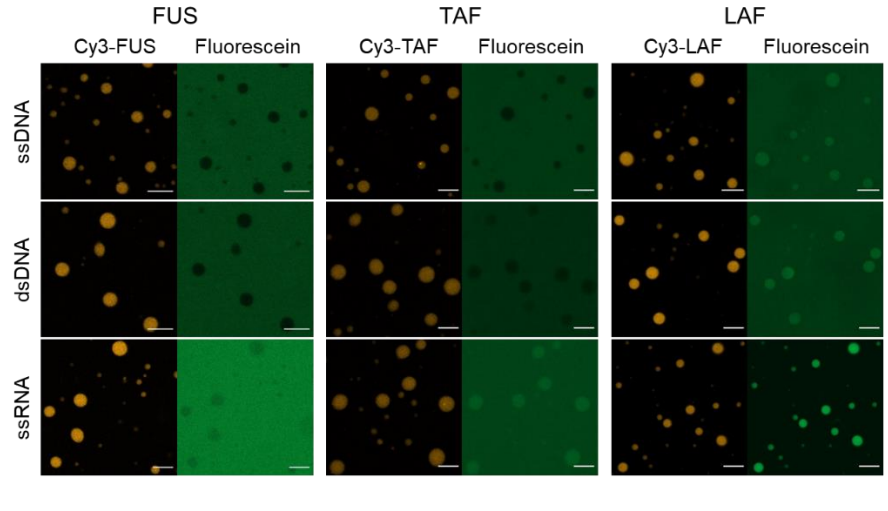

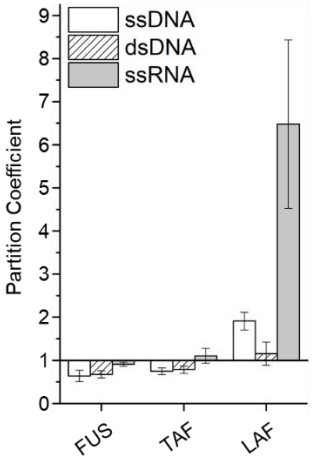

Scaffold	ssDNA	dsDNA	ssRNA
FUS	0.64 ± 0.13	0.67 ± 0.08	0.91 ± 0.05
TAF	0.75 ± 0.08	0.79 ± 0.09	1.10 ± 0.17
LAF	1.91 ± 0.21	1.15 ± 0.27	6.48 ± 1.95

Figure S10. Oligonucleotide (ON) recruitment to IDR droplets. Fluorescein (green) labeled single-stranded DNA (ssDNA), double-stranded DNA (dsDNA), and RNA (ssRNA) were added to three IDR droplets with Cy3-labeled scaffold IDRs. PC values are also summarized in the below table. Error bars: 1 s.d. (n = 100 from three independent experiments). Scale bars 10 μm.

.

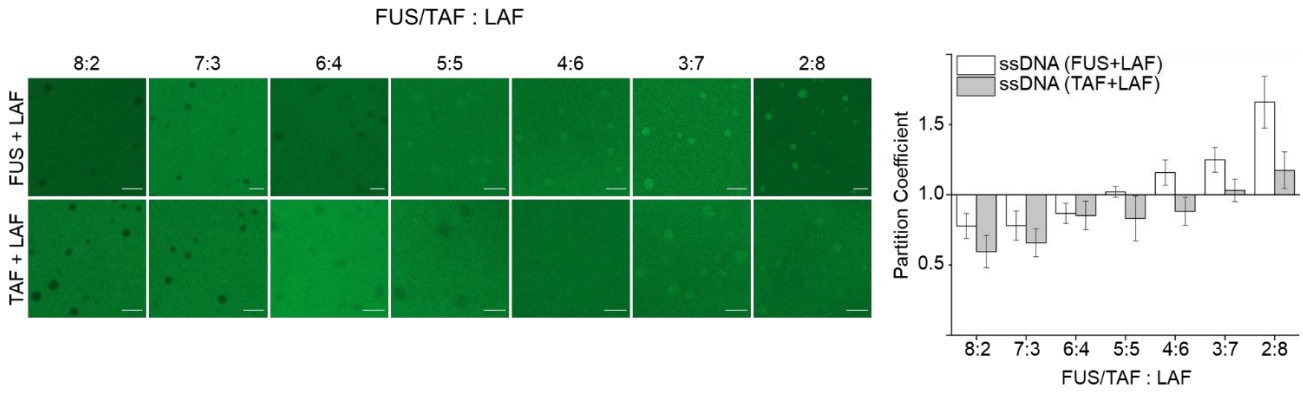

Figure S11. Control of DNA recruitment into IDR droplets by mixing varying ratios of two IDR scaffolds. Single-stranded DNA was added to IDR droplets that were formed with indicated ratios of two scaffold IDRs. Error bars: 1 s.d. (n = 100 from three independent experiments). Scale bars 10 μm.

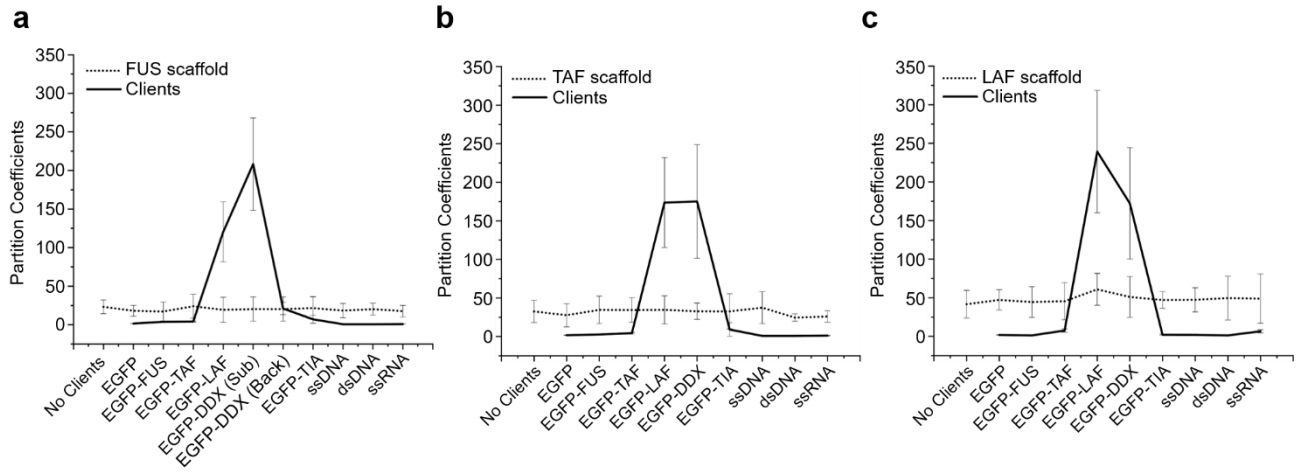

Figure S12. Partition coefficients of scaffold and client IDRs. PC values of scaffold IDR **(a)** FUS, **(b)** TAF, and **(c)** LAF IDRs in the presence of various client proteins and ONs are shown with dotted lines, while client PCs in these droplets are shown with solid lines. Error bars: 1 s.d. (n = 100 from three independent experiments).

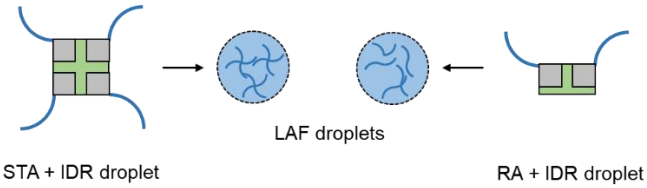

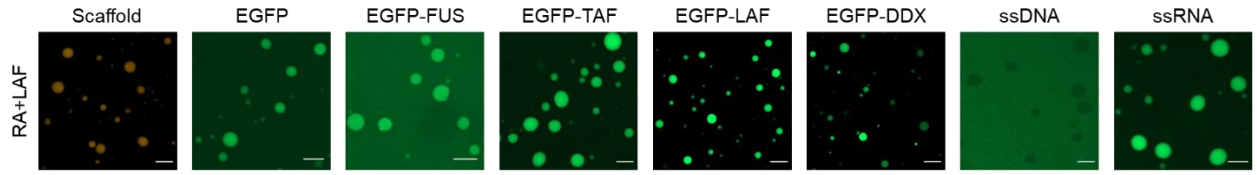

+RA	38.6 ± 18.4	2.0 ± 0.7	1.3 ± 0.1	4.2 ± 1.3	208.3 ± 71.1	104.6 ± 51.2	0.8 ± 0.1	3.4 ± 2.5
+STA	43.3 ± 19.7	1.8 ± 0.2	1.2 ± 0.1	7.5 ± 2.1	239.3 ± 79.5	172.3 ± 72.2	1.9 ± 0.2	6.5 ± 2.0

Figure S13. Recruitment of client IDRs into dimerization-induced IDR droplets by rhizavidin (RA). Fluorescence images of RA-induced LAF droplets with various client IDRs, free EGFP, and ONs. Partition coefficients are shown in the table with client PCs of STA-induced LAF droplets for comparison. N = 100 from three independent experiments. Scale bars 10 μm.

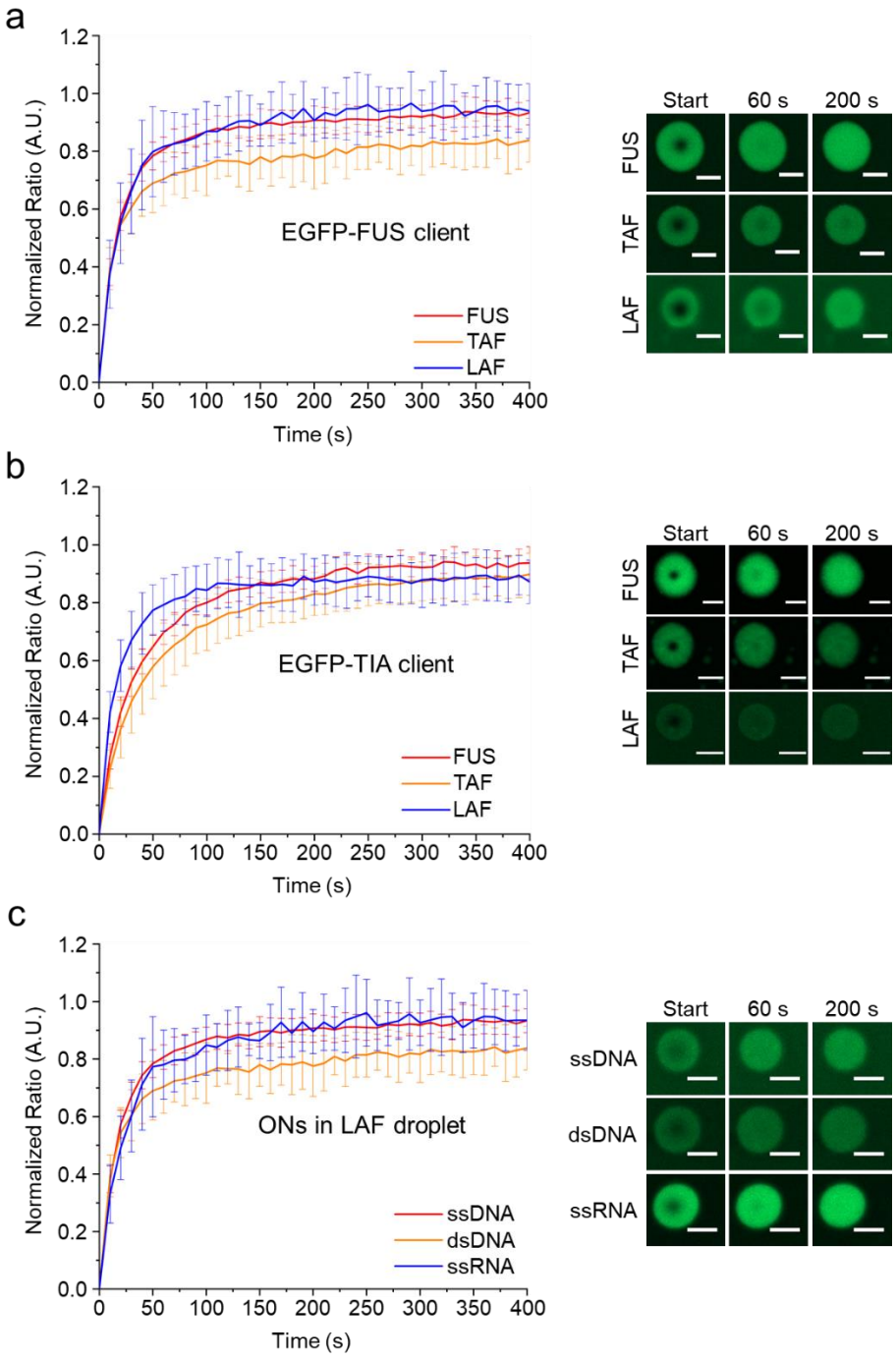

Figure S14. Diffusion of IDR clients and ONs inside IDR droplets. FRAP recovery curves and images of client EGFP-FUS **(a)**, EGFP-TIA **(b)**, and ONs (in LAF droplets) **(c)** were shown. Error bars: 1 s.d. (n = 15 from three independent experiments). Scale bars 5 μm.

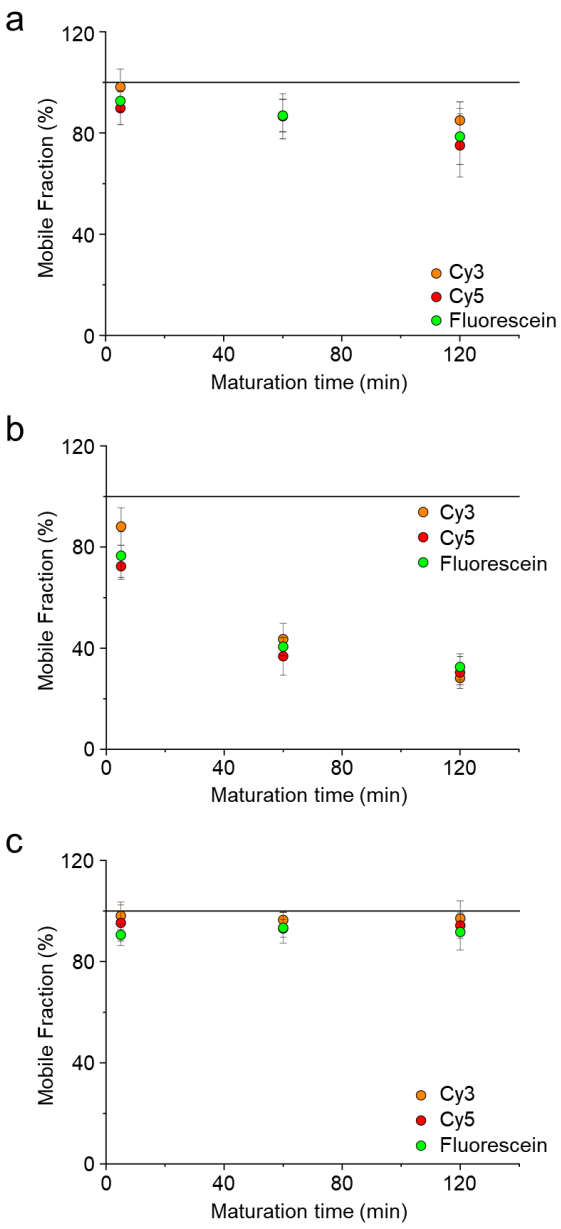

FUS Droplets

	5 min	60 min	120 min
Cy3	98.2 ± 7.1 %	86.9 ± 6.4 %	85.0 ± 7.3 %
Cy5	89.8 ± 6.5 %	86.6 ± 8.9 %	75.1 ± 12.5 %
Fluorescein	92.7 ± 4.1 %	86.9 ± 6.5 %	78.6 ± 11.1 %

TAF Droplets

	5 min	60 min	120 min
Cy3	88.1 ± 7.4 %	43.6 ± 6.2 %	28.2 ± 2.7 %
Cy5	72.4 ± 4.4 %	36.8 ± 7.5 %	30.4 ± 6.3 %
Fluorescein	76.6 ± 9.3 %	40.6 ± 3.6 %	32.6 ± 5.2 %

LAF Droplets

	5 min	60 min	120 min
Cy3	98.1 ± 5.4 %	96.5 ± 2.9 %	97.1 ± 6.9 %
Cy5	95.3 ± 7.1 %	93.1 ± 3.5 %	94.3 ± 5.1 %
Fluorescein	90.6 ± 4.2 %	93.4 ± 6.1 %	91.7 ± 7.1 %

Figure S15. Maturation of IDR droplets. Mobile fractions of IDR droplets (FUS, TAF, LAF) were measured at 5 min, 60 min, and 120 min after droplet formation (maturation time). Error bars: 1 s.d. (n = 15 from three independent experiments).

Note: Three different dyes (Cy3, Cy5, and fluorescein) were used to label scaffold IDRs and their mobile fractions measured. The data indicate that IDR mobility was not affected by the nature of conjugated dyes.

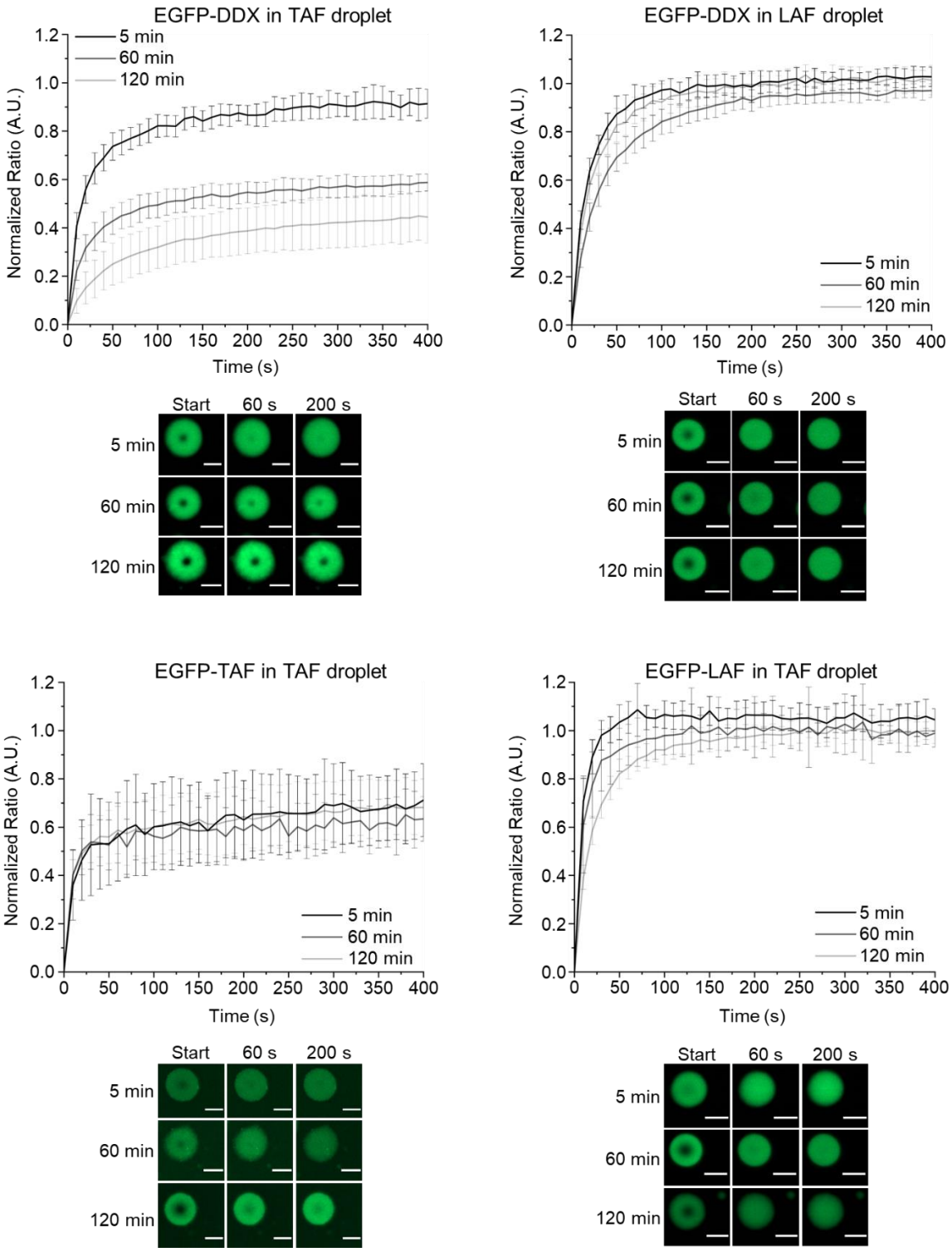

Figure S16. Diffusion of IDR clients inside differently matured IDR droplets. FRAP recovery curves and images of indicated client IDRs in indicated droplets were shown. Error bars: 1 s.d. (n = 15 from three independent experiments). Scale bars 5 μm.

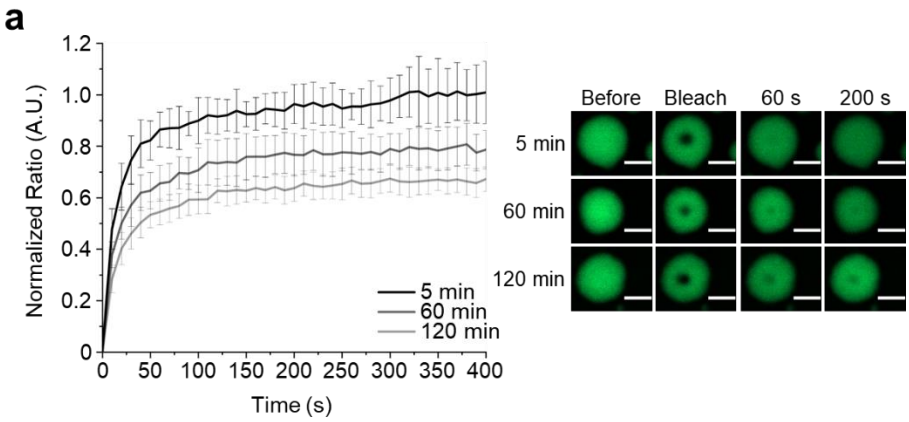

b

EGFP-DDX-CS	5 min	60 min	120 min
Mobile Fraction (%)	96.2 ± 7.4	77.1 ± 7.3	65.1 ± 4.5
$t_{1/2}$ (s)	14.6 ± 3.8	16.3 ± 2.4	18.8 ± 4.2

EGFP-DDX	5 min	60 min	120 min
Mobile Fraction (%)	91.4 ± 6.0	64.3 ± 21.1	44.4 ± 10.0
$t_{1/2}$ (s)	32.8 ± 19.4	38.0 ± 19.1	79.6 ± 26.2

Figure S17. Diffusion of charge-scrambled DDX inside differently matured TAF droplets. (a) FRAP recovery curves and images of charge-scrambled client DDX (EGFP-DDX-CS) in TAF droplets. Error bars: 1 s.d. (n = 15 from three independent experiments). Scale bars 5 μm. (b) The mobile fractions and diffusion half times of EGFP-DDX-CS and wild-type EGFP-DDX (from Figure S16).

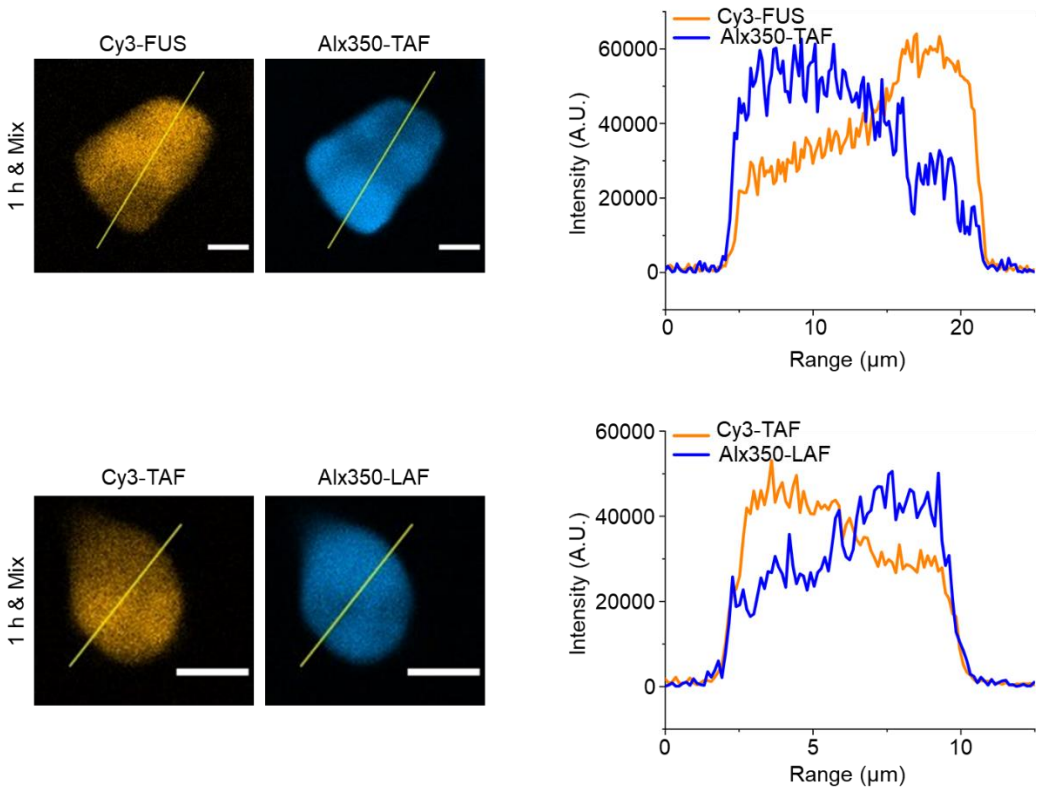

Figure S18. Fluorescence images and intensity profiles of multiphase droplets containing two scaffold IDRs. Fluorescence profiles are obtained through the yellow lines that across multiphase droplets. Scale bars 5 μm.

Note: Segregation boundaries, which separate dense and diluted phases, were defined by where two fluorescence profiles intersect.

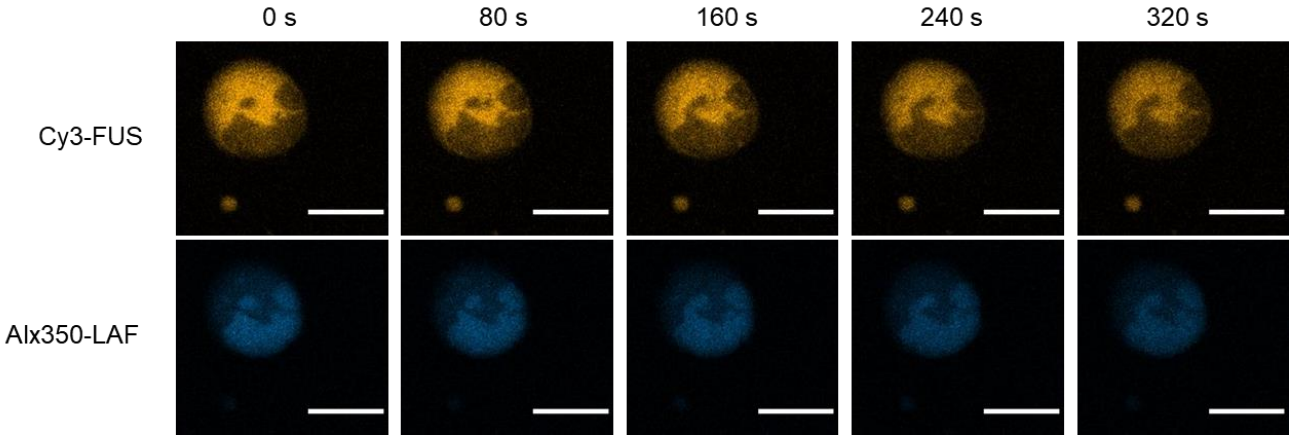

Figure S19. Fusion of segregated phases inside a FUS+LAF multiphase droplet. Dense parts of LAF slowly fused with each other as shown in the bottom blue images. Scale bars 10 μm.

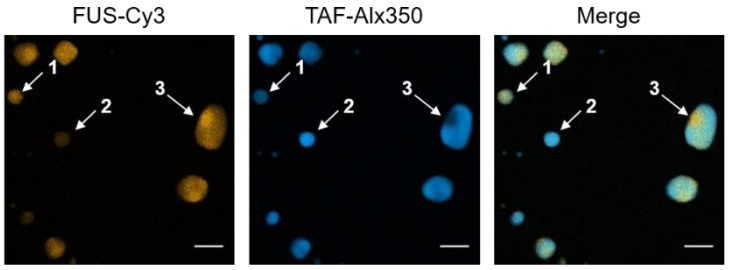

Uniform distribution				Segregation	
Type 1 High FUS signal		Type 2 High TAF signal		Type 3 Segregated signal	
20% (24/121)		57% (69/121)		23% (28/121)	
Ratio (Alx350/Cy3) (TAF/FUS)	Size (μm^2)	Ratio (Alx350/Cy3) (TAF/FUS)	Size (μm^2)	Ratio (Alx350/Cy3) (TAF/FUS)	Size (μm^2)
0.73 ± 0.19	21.6 ± 16.7	2.20 ± 1.04	24.2 ± 21.0	1.02 ± 0.27	90.0 ± 59.0

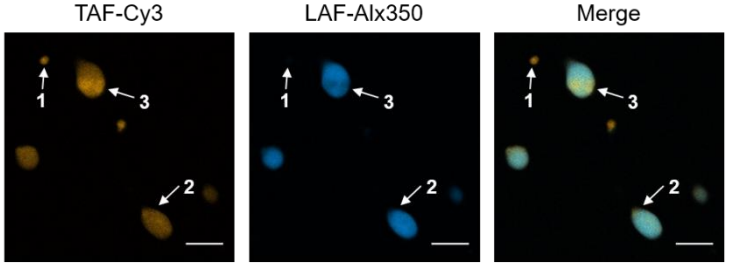

Uniform distribution				Segregation	
Type 1 High TAF signal		Type 2 High LAF signal		Type 3 Segregated signal	
24% (31/132)		54% (71/132)		23% (30/132)	
Ratio (Alx350/Cy3) (LAF/TAF)	Size (μm^2)	Ratio (Alx350/Cy3) (LAF/TAF)	Size (μm^2)	Ratio (Alx350/Cy3) (LAF/TAF)	Size (μm^2)
0.56 ± 0.28	13.3 ± 10.0	1.96 ± 0.95	21.0 ± 18.8	1.04 ± 0.30	68.6 ± 31.3

Figure S20. Analysis of FUS+TAF (top) and TAF+LAF (bottom) droplet mixture. Droplets were matured 1 h before mixing. Representative droplets of uniformly distributed droplets with high Cy3 (type 1) or high Alx350 (type 2) signals and segregated droplets (type 3) are indicated with arrows and numbers. Population, relative IDR ratios, and sizes of these three types of droplets are summarized in below tables. (n=121 for FUS+TAF and n=132 for TAF+LAF from 5 independent experiments). Scale bars 10 μm.

Note I: Uneven IDR ratios of type 1 and type 2 droplets (0.73-2.20 and 0.56-1.96) are less apparent compared to FUS+LAF droplet mixtures (0.32-4.49), likely because many FUS+TAF and TAF+LAF droplet-droplet fusion products with even IDR population do not form segregated droplets, unlike the FUS+LAF mixture.

Note II: Based on relative portions of type 1 and type 2 droplets for all three cases of IDR mixtures, droplets with high LAF signals are most abundant, while droplets with high FUS signals are least abundant (LAF > TAF > FUS), likely indicating that higher number of LAF droplets are generated by LLPS. This trend is similar to the droplet enrichment propensity (LAF > TAF > FUS in Figure 2).

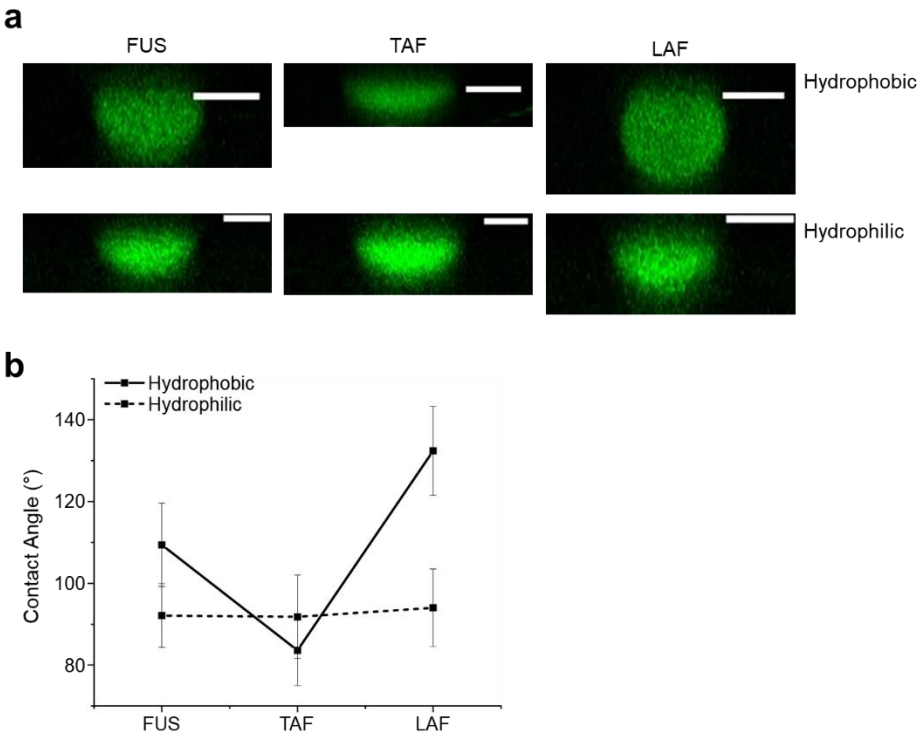

Figure S21. Comparison of IDR droplet surface tensions. (a) Fluorescence images of IDR droplets on hydrophobic (Silanized, top) or hydrophilic (bare, bottom) glasses. Fluorescein-tagged scaffolds (2 μM) were mixed with IDR scaffolds to visualize droplet shapes on surfaces. Scale bar = 5 μm. **(b)** Line plots of IDR droplet contact angles (n = 60 from three independent experiments).

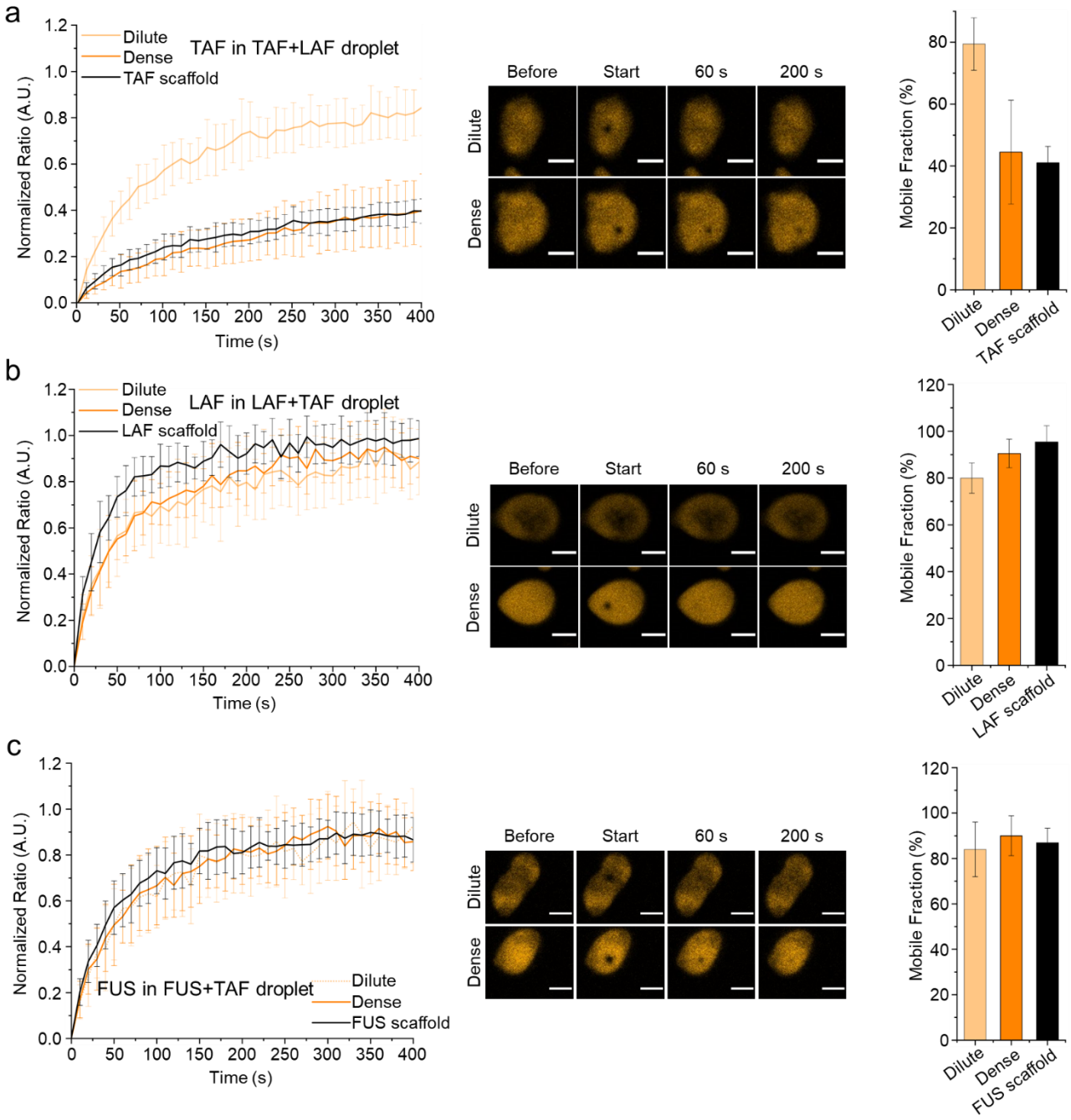

Figure S22. Dynamic diffusion of scaffold IDRs inside multiphase droplets. FRAP recovery curves and images of dense and diluted phases of TAF in TAF+LAF droplets **(a)**, LAF in LAF+TAF droplets **(b)**, and FUS in FUS+TAF droplets **(c)** are shown. Black curves are scaffold FRAP recoveries of single IDR droplets after 1 h maturation (Figure 3a). Mobile fractions were also shown in the right graphs. Error bars: 1 s.d. (n = 15). Scale bars 5 μm.

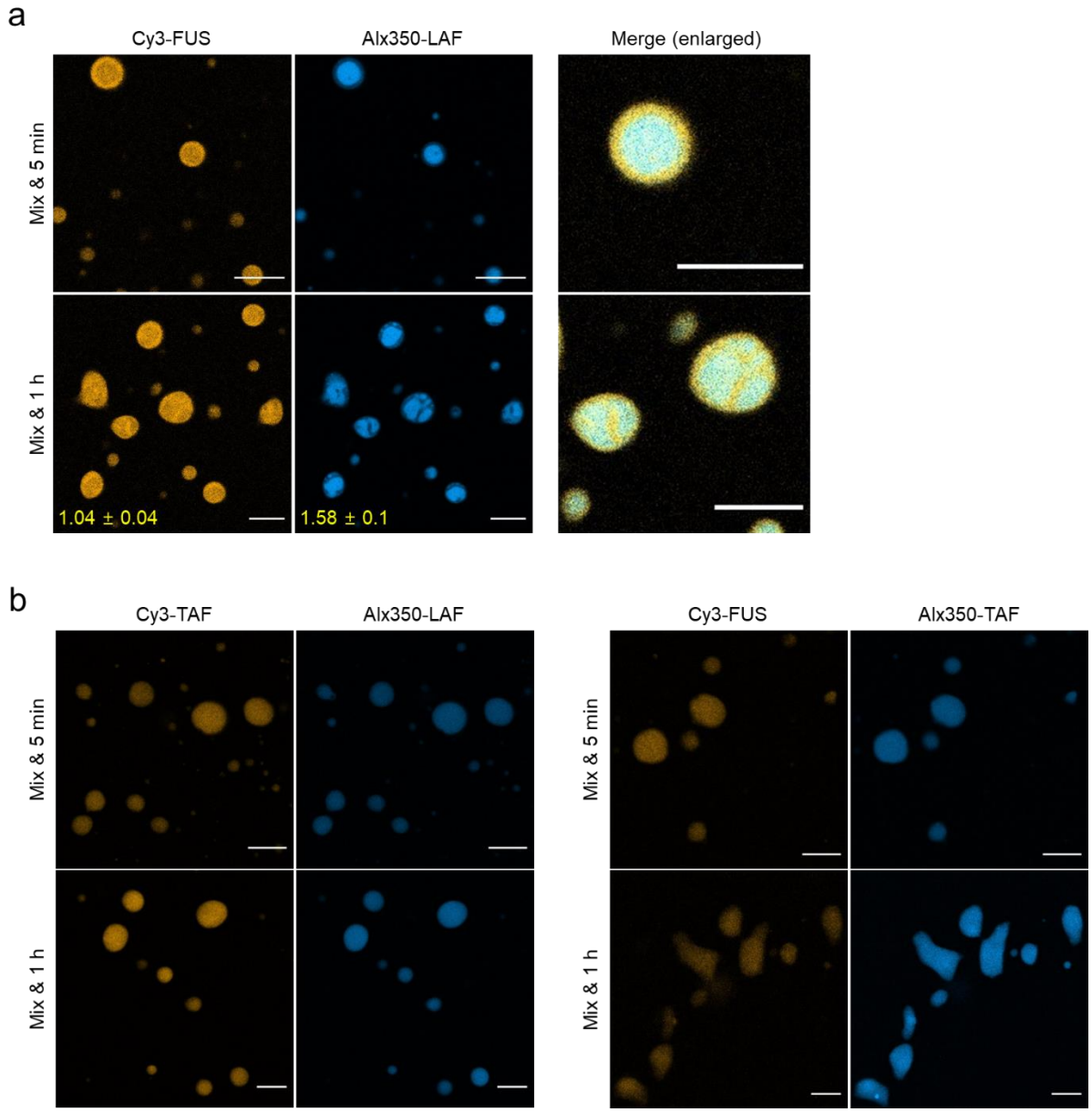

Figure S23. Droplet formation of pre-mixed two scaffold IDRs. (a) STA-bound Biotin-SUMO-FUS and biotin-SUMO-LAF were mixed first, and droplet formation was induced by PEG addition. Images were obtained after 5 min or 1 h maturation. Enlarged merge images are shown in right. **(b)** Droplet formation of pre-mixed TAF/LAF (left) or FUS/TAF (right) scaffold IDRs. Scale bars 10 μm.

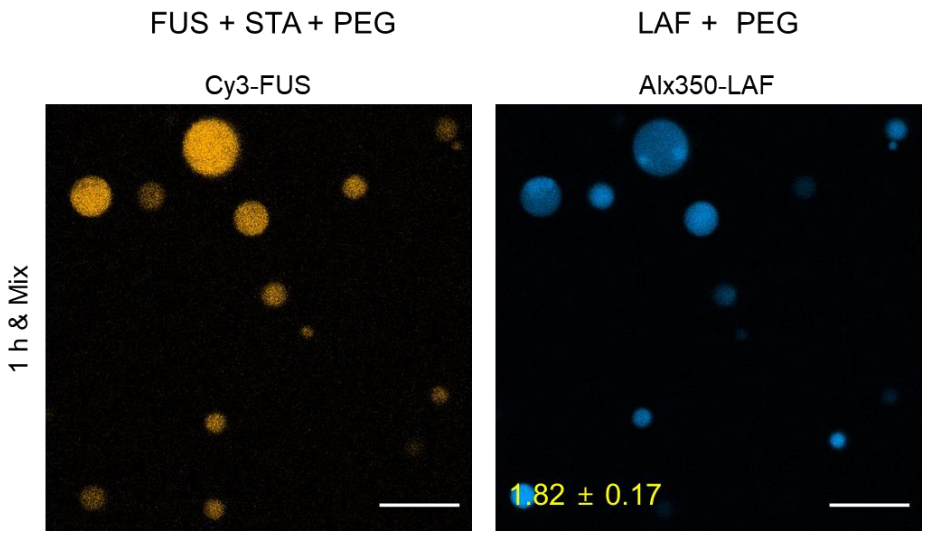

Figure S24. Droplet interactions between clustered FUS droplets and monomeric LAF droplets. LAF droplets were generated by only adding PEG without STA clustering, and mixed with FUS droplets. Scale bars 10 μm.

Table S1. Partition coefficients of Figure 2.

	Scaffold	EGFP-FUS	EGFP-TAF	EGFP-LAF	EGFP-DDX	EGFP-TIA	EGFP
FUS	23.2 ± 8.9	3.9 ± 0.7	4.2 ± 0.8	120.4 ± 39.0	208.2 ± 60.0 21.0 ± 7.8	12.0 ± 3.4	1.5 ± 0.1
TAF	32.5 ± 14.3	2.7 ± 0.8	4.3 ± 1.0	173.7 ± 58.3	175.1 ± 73.7	19.6 ± 8.9	1.7 ± 0.1
LAF	43.3 ± 19.7	1.2 ± 0.1	7.5 ± 2.1	239.3 ± 79.5	172.3 ± 72.2	2.6 ± 0.7	1.8 ± 0.2

Table S2. Mobile fractions (top) and $t_{1/2}$ (bottom) of Figure 3.

	No Clients	EGFP-FUS	EGFP-TAF	EGFP-LAF	EGFP-DDX	EGFP-TIA
FUS	86.9 ± 6.4 %	90.1 ± 4.8 %	93.0 ± 2.7 %	95.7 ± 8.3 %	30.2 ± 4.4 % 84.9 ± 5.7 %	92.2 ± 4.2 %
TAF	36.4 ± 7.1 %	79.6 ± 6.6 %	75.3 ± 4.7 %	99.8 ± 5.2 %	64.3 ± 21.1 %	88.9 ± 9.3%
LAF	95.4 ± 7.0 %	92.6 ± 7.9 %	92.0 ± 6.8 %	98.1 ± 3.6 %	97.4 ± 4.6 %	88.0 ± 7.7 %
	No Clients	**EGFP-FUS**	**EGFP-TAF**	**EGFP-LAF**	**EGFP-DDX**	**EGFP-TIA**
FUS	38.9 ± 13.7 s	15.8 ± 2.0 s	16.8 ± 2.4 s	16.3 ± 3.8 s	53.2 ± 19.5 s 30.9 ± 5.9 s	28.3 ± 3.5 s
TAF	79.7 ± 15.8 s	15.8 ± 2.8 s	12.8 ± 2.7 s	10.8 ± 3.0 s	38.0 ± 19.1 s	52.6 ± 10.3 s
LAF	29.6 ± 6.8 s	23.7 ± 7.7 s	18.9 ± 3.6 s	14.0 ± 3.9 s	21.7 ± 6.4 s	17.3 ± 3.5 s

Protein sequences

AP-FUS (Underline: FUS IDR, Red: 6xHis tag, Blue: TEV protease site, Green: AP tag)

MSYYHHHHHHDYDIPTTENLYFQGAMDGGLNDIFEAQKIEWHEASNDYTQQATQSYGAYPTQPGQGYSQQSSQ
PYGQQSYSGYSQSTDTSGYGQSSYSSYGQSQNTGYGTQSTPQGYGSTGGYGSSQSSQSSYGQQSSYPGYGQQP
APSSTSGSYGSSSQSSSYGQPQSGSYSQQPSYGGQQQSYGQQQSYNPPQGYGQQNQYNSSSGGGGGGGGGGNY
GQDQSSMSSGGGSGGGYGNQDQSGGGGSGGYGQQDRG

AP-SUMO-FUS (Underline: FUS IDR, Red: 6xHis tag, Blue: TEV protease site, Green: AP tag, Gray: SUMO)

MSYYHHHHHHDYDIPTTENLYFQGAMEGLNDIFEAQKIEWHEMSDSEVNQEAKPEVKPEVKPETHINLKVSDG
SSEIFFKIKKTTPLRRLMEAFAKRQGKEMDSLRFLYDGIRIQADQTPEDLDMEDNDIIEAHREQIGGATYEFA
SNDYTQQATQSYGAYPTQPGQGYSQQSSQPYGQQSYSGYSQSTDTSGYGQSSYSSYGQSQNTGYGTQSTPQGY
GSTGGYGSSQSSQSSYGQQSSYPGYGQQPAPSSTSGSYGSSSQSSSYGQPQSGSYSQQPSYGGQQQSYGQQQS
YNPPQGYGQQNQYNSSSGGGGGGGGGGNYGQDQSSMSSGGGSGGGYGNQDQSGGGGSGGYGQQDRG

AP-SUMO-TAF (Underline: TAF IDR, Red: 6xHis tag, Blue: TEV protease site, Green: AP tag, Gray: SUMO)

MSYYHHHHHHDYDIPTTENLYFQGAMEGLNDIFEAQKIEWHEMSDSEVNQEAKPEVKPEVKPETHINLKVSDG
SSEIFFKIKKTTPLRRLMEAFAKRQGKEMDSLRFLYDGIRIQADQTPEDLDMEDNDIIEAHREQIGGATYEFM
SDSGSYGQSGGEQQSYSTYGNPGSQGYGQASQSYSGYGQTTDSSYGQNYSGYSSYGQSQSGYSQSYGGYENQK
QSSYSQQPYNNQGQQQNMESSGSQGGRAPSYDQPDYGQQDSYDQQSGYDQHQGSYDEQSNYDQQHDSYSQNQQ
SYHSQRENYSHHTQDDRRDVSRYGEDNRGYGGSQGGGRGRGGYDKDGRGPMTGSSGGDRGG

AP-SUMO-LAF (Underline: LAF IDR, Red: 6xHis tag, Blue: TEV protease site, Green: AP tag, Gray: SUMO)

MSYYHHHHHHDYDIPTTENLYFQGAMEGLNDIFEAQKIEWHEMSDSEVNQEAKPEVKPEVKPETHINLKVSDG
SSEIFFKIKKTTPLRRLMEAFAKRQGKEMDSLRFLYDGIRIQADQTPEDLDMEDNDIIEAHREQIGGATYEFM
ESNQSNNGGSGNAALNRGGRYVPPHLRGGDGGAAAAASAGGDDRRGGAGGGGYRRGGGNSGGGGGGGYDRGYN
DNRDDRDNRGGSGGYGRDRNYEDRGYNGGGGGGGNRGYNNNRGGGGGGYNRQDRGDGGSSNFSRGGYNNRDEG
SDNRGSGRSYNNDRRDNGGDG

EGFP (Red: 6xHis tag)

MMVSKGEELFTGVVPILVELDGDVNGHKFSVSGEGEGDATYGKLTLKFICTTGKLPVPWPTLVTTLTYGVQCF
SRYPDHMKQHDFFKSAMPEGYVQERTIFFKDDGNYKTRAEVKFEGDTLVNRIELKGIDFKEDGNILGHKLEYN
YNSHNVYIMADKQKNGIKVNFKIRHNIEDGSVQLADHYQQNTPIGDGPVLLPDNHYLSTQSALSKDPNEKRDH
MVLLEFVTAAGITLGMDELYKLEHHHHHH

EGFP-FUS (Underline: FUS IDR, Red: 6xHis tag, Green: EGFP)

MMVSKGEELFTGVVPILVELDGDVNGHKFSVSGEGEGDATYGKLTLKFICTTGKLPVPWPTLVTTLTYGVQCF
SRYPDHMKQHDFFKSAMPEGYVQERTIFFKDDGNYKTRAEVKFEGDTLVNRIELKGIDFKEDGNILGHKLEYN
YNSHNVYIMADKQKNGIKVNFKIRHNIEDGSVQLADHYQQNTPIGDGPVLLPDNHYLSTQSALSKDPNEKRDH
MVLLEFVTAAGITLGMDELYKEFASNDYTQQATQSYGAYPTQPGQGYSQQSSQPYGQQSYSGYSQSTDTSGYG
QSSYSSYGQSQNTGYGTQSTPQGYGSTGGYGSSQSSQSSYGQQSSYPGYGQQPAPSSTSGSYGSSSQSSSYGQ
PQSGSYSQQPSYGGQQQSYGQQQSYNPPQGYGQQNQYNSSSGGGGGGGGGGNYGQDQSSMSSGGGSGGGYGNQ
DQSGGGGSGGYGQQDRGLEHHHHHH

EGFP-TAF (Underline: TAF IDR, Red: 6xHis tag, Green: EGFP)

MMVSKGEELFTGVVPILVELDGDVNGHKFSVSGEGEGDATYGKLTLKFICTTGKLPVPWPTLVTTLTYGVQCF
SRYPDHMKQHDFFKSAMPEGYVQERTIFFKDDGNYKTRAEVKFEGDTLVNRIELKGIDFKEDGNILGHKLEYN
YNSHNVYIMADKQKNGIKVNFKIRHNIEDGSVQLADHYQQNTPIGDGPVLLPDNHYLSTQSALSKDPNEKRDH

MVLLEFVTAAGITLGMDELYKEFMSDSGSYGQSGGEQQSYSTYGNPGSQGYGQASQSYSGYGQTTDSSYGQNY
SGYSSYGQSQSGYSQSYGGYENQKQSSYSQQPYNNQGQQQNMESSGSQGGRAPSYDQPDYGQQDSYDQQSGYD
QHQGSYDEQSNYDQQHDSYSQNQQSYHSQRENYSHHTQDDRRDVSRYGEDNRGYGGSQGGGRGRGGYDKDGRG
PMTGSSGGDRGGLEHHHHHH

EGFP-LAF (Underline: LAF IDR, Red: 6xHis tag, Green: EGFP)
MMVSKGEELFTGVVPILVELDGDVNGHKFSVSGEGEGDATYGKLTLKFICTTGKLPVPWPTLVTTLTYGVQCF
SRYPDHMKQHDFFKSAMPEGYVQERTIFFKDDGNYKTRAEVKFEGDTLVNRIELKGIDFKEDGNILGHKLEYN
YNSHNVYIMADKQKNGIKVNFKIRHNIEDGSVQLADHYQQNTPIGDGPVLLPDNHYLSTQSALSKDPNEKRDH
MVLLEFVTAAGITLGMDELYKEFMESNQSNNGGSGNAALNRGGRYVPPHLRGGDGGAAAAASAGGDDRRGGAG
GGGYRRGGGNSGGGGGGGYDRGYNDNRDDRDNRGGSGGYGRDRNYEDRGYNGGGGGGGNRGYNNNRGGGGGGY
NRQDRGDGGSSNFSRGGYNNRDEGSDNRGSGRSYNNDRRDNGGDGLEHHHHHH

EGFP-LAF-CR (Underline: LAF IDR, Red: 6xHis tag, Green: EGFP)
MMVSKGEELFTGVVPILVELDGDVNGHKFSVSGEGEGDATYGKLTLKFICTTGKLPVPWPTLVTTLTYGVQCF
SRYPDHMKQHDFFKSAMPEGYVQERTIFFKDDGNYKTRAEVKFEGDTLVNRIELKGIDFKEDGNILGHKLEYN
YNSHNVYIMADKQKNGIKVNFKIRHNIEDGSVQLADHYQQNTPIGDGPVLLPDNHYLSTQSALSKDPNEKRDH
MVLLEFVTAAGITLGMDELYKEFMESNQSNNGGSGNAALNYGGSYVPPHLYGGYGGAAAAASAGGSSSYGGAG
GGGYSSGGGNSGGGGGGGYSSGYNSNSSSYSNSGGSGGYGSSSNYESSGYNGGGGGGGNSGYNNNSGGGGGGY
NSQSSGYGGSSNFSSGGYNNSSEGSYNSGSGSSYNNSSSYNGGSGLEHHHHHH

EGFP-DDX (Underline: DDX IDR, Red: 6xHis tag, Green: EGFP)
MMVSKGEELFTGVVPILVELDGDVNGHKFSVSGEGEGDATYGKLTLKFICTTGKLPVPWPTLVTTLTYGVQCF
SRYPDHMKQHDFFKSAMPEGYVQERTIFFKDDGNYKTRAEVKFEGDTLVNRIELKGIDFKEDGNILGHKLEYN
YNSHNVYIMADKQKNGIKVNFKIRHNIEDGSVQLADHYQQNTPIGDGPVLLPDNHYLSTQSALSKDPNEKRDH
MVLLEFVTAAGITLGMDELYKEFELRRQACGRMGDEDWEAEINPHMSSYVPIFEKDRYSGENGDNFNRTPASS
SEMDDGPSRRDHFMKSGFASGRNFGNRDAGECNKRDNTSTMGGFGVGKSFGNRGFSNSRFEDGDSSGFWRESS
NDCEDNPTRNRGFSKRGGYRDGNNSEASGPYRRGGRGSFRGCRGGFGLGSPNNDLDPDECMQRTGGLFGSRRP
VLSGTGNGDTSQSRSGSGSERGGYKGLNEEVITGSGKNSWKSEAEGGESLEHHHHHH

EGFP-DDX-CS (Underline: DDX-CS IDR, Red: 6xHis tag, Green: EGFP)
MMVSKGEELFTGVVPILVELDGDVNGHKFSVSGEGEGDATYGKLTLKFICTTGKLPVPWPTLVTTLTYGVQCF
SRYPDHMKQHDFFKSAMPEGYVQERTIFFKDDGNYKTRAEVKFEGDTLVNRIELKGIDFKEDGNILGHKLEYN
YNSHNVYIMADKQKNGIKVNFKIRHNIEDGSVQLADHYQQNTPIGDGPVLLPDNHYLSTQSALSKDPNEKRDH
MVLLEFVTAAGITLGMDELYKEFELRRQACGRMGDRDWRAEINPHMSSYVPIFEKDRYSGENGRNFNDTPASS
SEMRDGPSERDHFMKSGFASGDNFGNRDAGKCNERDNTSTMGGFGVGKSFGNEGFSNSRFERGDSSGFWRESS
NDCRDNPTRNDGFSDRGGYEKGNNSEASGPYERGGRGSFDGCRGGFGLGSPNNRLDPRECMQRTGGLFGSDRP
VLSGTGNGDTSQSRSGSGSERGGYKGLNEKVITGSGENSWKSEARGGESLEHHHHHH

EGFP-TIA (Underline: TIA IDR, Red: 6xHis tag, Green: EGFP)
MMVSKGEELFTGVVPILVELDGDVNGHKFSVSGEGEGDATYGKLTLKFICTTGKLPVPWPTLVTTLTYGVQCF
SRYPDHMKQHDFFKSAMPEGYVQERTIFFKDDGNYKTRAEVKFEGDTLVNRIELKGIDFKEDGNILGHKLEYN
YNSHNVYIMADKQKNGIKVNFKIRHNIEDGSVQLADHYQQNTPIGDGPVLLPDNHYLSTQSALSKDPNEKRDH
MVLLEFVTAAGITLGMDELYKEFINPVQQQNQIGYPQPYGQWGQWYGNAQQIGQYMPNGWQVPAYGMYGQAWN
QQGFNQTQSSAPWMGPNYGVQPPQGQNGSMLPNQPSGYRVAGYETQLEHHHHHH

Experimental methods

Protein preparation. Biotin-tagged FUS and various Biotin-SUMO-tagged IDR genes were cloned into the pProExHTα expression vector (Invitrogen), and the plasmids were transformed in AVB101 (Avidity), an *E.coli* B strain (hsdR, lon11, SulA1) containing a pACYC184 plasmid, which produces biotin ligase BirA. The transformed cells were grown at 37 °C until OD600 reaches 0.8, and proteins were induced with 0.05 mM biotin and 1 mM Isopropyl β-D-1-thiogalactopyranoside (IPTG), followed by incubation at 37 °C for 6 h. After IPTG induction, cells were harvested by centrifugation at 6000 rpm for 5 min. The cells were lysed by sonication in the storage buffer (200 mM NaCl, 50 mM Tris pH 8.0, 1 mM EDTA, 10% Glycerol). Lysed cells were then centrifuged at 12000 rpm for 15 min at 4 °C, and the supernatants were purified by Ni-IDA columns (BioProgen, Daejeon, South Korea). Purified proteins were dialyzed into storage buffer at 25 °C, and centrifugally concentrated by Vivaspin 20 columns with a 10 kDa molecular weight cutoff (GE Healthcare) until the protein concentrations reach the range 150~200 μM (LAF), and 250~300 μM (FUS, TAF). Concentrated proteins were incubated at 60 °C with a heat block (ALB6400, FINEPCR Co.) for 20 min to remove impurities by selective aggregation of non-specific proteins. Aggregates were centrifuged, and further purified IDR proteins were finally filtrated through a 0.2 μm membrane filter (Advantec, DISMIC-13 CP). Final protein concentrations were measured by A280, and protein samples were flash-frozen by liquid nitrogen and stored in -80 °C.

Free EGFP and EGFP-tagged IDR genes were cloned into the pET-21a expression vector (EMD Biosciences), and the plasmids were transformed in E.coli BL21 (DE3). The transformed cells were grown at 37 °C until OD600 reaches 0.8, and proteins were induced with 1 mM IPTG and then incubated at 37 °C for 6 h, except EGFP-TIA, which is induced at 20 °C for 18 h. Proteins were similarly purified by Ni-IDA columns. EGFP-DDX and EGFP-TIA were additionally purified by ion-exchange chromatography (Q Excellose, BioProgen). Final protein concentrations were measured by A280, and protein samples were flash-frozen by liquid nitrogen and stored in -80 °C.

Streptavidin (STA) and Rhizavidin (RA) genes were cloned into the pET-21a expression vector (EMD Biosciences), and the plasmids were transformed in E.coli BL21 (DE3). The transformed cells were grown at 37 °C until OD600 reaches 0.8, and proteins were induced with 1 mM IPTG and then incubated at 37 °C for 4 h. After IPTG induction, cells were harvested and lysed by sonication in a PBS buffer containing 0.1% Triton X-100. Lysed cells were then centrifuged at 12000 rpm for 15 min at 4 °C, and the soluble proteins were discarded. The pellets were completely re-suspended in PBS buffer containing 0.1% Triton X-100 and centrifuged again at 12000 rpm for 15 min at 4 °C. The

washed inclusion bodies were dissolved in 15 mL of 6 M Guanidine hydrochloride (GuHCl) and 50 mM Tris-HCl (pH 8.0) for overnight at 4 °C. Remained insoluble proteins were then removed by centrifugation at 12000 rpm for 30 min at 4 °C.

For refolding, denatured STA and RA proteins were diluted dropwise into 200 mL of PBS until solutions become turbid. When solutions became turbid, aggregations were removed by centrifugation at 6000 rpm, 4 °C for 30 min and filtered through a 0.22 μm membrane filter (Stericup® Quick Release, Millipore Express® PLUS). The solutions were maintained at 4 °C for overnight. After overnight, the refolded solutions were added 100 mM NaCl and 50 mM Tris-HCl (pH 8.0) and purified by Ni-IDA columns (BioProgen). The final products were dialyzed into the storage buffer and stored at -20 °C.

Fluorescent dye labelling of IDR proteins. Scaffold proteins (FUS, TAF, LAF) were labelled with Cyanine 3 (Cy3), Cyanine 5 (Cy5), Fluorescein, and Alexa Fluor 350 by NHS ester conjugations. Proteins were dialyzed in the labelling buffer (200 mM NaCl, 10% Glycerol) and mixed with dyes in 1 : 0.5 protein/dye ratio. The mixed solutions were incubated for 30 min at 25 °C with shaking (SLRM-3, SeouLin Bioscience), and dye-conjugated proteins were purified by PD10 desalting columns (Sephadex™ G-25 M, GE Healthcare). Concentrations of labelled proteins were measured by A280, and concentrations of proteins with Alexa Fluor 350 were quantified by absorbance at 346 nm (19000 $M^{-1}cm^{-1}$).

Liquid droplet formation and observation. Stored proteins were thawed at 34 °C for 20 min. Solutions with aggregation were filtrated through a 0.2 μm membrane filter (Advantec, DISMIC-13 CP), and the concentration was measured again by A280. For droplet formation, intact scaffold proteins were mixed with fluorescent dye-conjugated scaffold proteins in 1.5 mL Eppendorf (ep) tube. The final total concentration of scaffolds was 80 μM (Biotin-SUMO-FUS, TAF) or 60 μM (Biotin-SUMO-LAF), and the dye-tagged scaffolds proportion was ~ 2 μM.

STA or RA was mixed in a 1:1 molecule ratio with scaffold proteins to make multivalent IDR clusters, and final 15% (or 1.5%) weight poly-ethylene glycol (PEG, molecular weight 8000, LPS solution) in distilled water was mixed to induce phase separation. Final buffer condition after PEG mixing was 110 mM NaCl, 27.5 mM Tris pH 8.0, 5.5% Glycerol, and 0.55 mM EDTA. When the solutions became turbid, clients were added to the solution in 80:1 ratio against scaffold proteins. Mixed solutions were maintained for 5 min in tubes. For confocal analysis, 5 μL of solutions with droplets were dropped on a hydrophobic modified slide glass and covered by a cover glass. For hydrophobic coating of glass surfaces, slide glasses (Marienfeld) and cover glasses (Duran) were

immersed to the piranha acid solution (95% Sulfuric acid 450 mL + 35% Hydrogen peroxide 150 mL) and incubated for 1 h at 60 °C. The glasses were serially washed by distilled water and acetone, and blew by nitrogen gas. The glasses were immersed to the coating solution (5 mL 3-(Trimethoxysilyl)propylmethacrylate, 10 mL acetic acid, and 35 mL acetone) and incubated with shaking on an orbital shaker (SH30, FINEPCR) at 25 °C for 2 h. The glasses were again washed by acetone and distilled water and blew by nitrogen gas. The glasses were stored in a dry keeper (SANPLATEC co.) and used in 48 h.

The cover glasses with solutions were sealed by nail polish and observed by LSM 800 laser scanning confocal microscope (Carl Zeiss, LSM800). Fluorescent images and DIC images were all processed by the Image J (National institutes of Health) software. Most droplet observations and experiments were processed on hydrophobic glasses to prevent the droplet moving during FRAP analysis. However, droplet fusion (Fig. 1c) and EGFP-DDX subcompartment formation (Fig. S5) were observed in a 15μ-Slide 18 well plate (Ibidi®, uncoated) with BSA coating on the surface by loading 10 mg/ml BSA for overnight at 4 °C. Coomassie-blue gel images (Figure S1a and Figure S3) in 15% SDS-PAGE gels (containing 0.01% SDS) were acquired by Chemi-doc (Biorad).

Partition coefficient (PC) analysis. Fluorescence mean intensities inside droplets (scaffolds and recruited clients) were measured from droplets with >1 μm diameters. For the fluorescence mean intensity outside droplets, the average signal of the most abundant intensity was first obtained, and a mean fluorescent signal within 95% (1.96σ) of the average signal was measured as the outside mean intensity. PCs were obtained by dividing inside droplet mean intensities of selected droplets with the outside mean intensity. 100 droplets from at least 3 independent experiments were selected for partition coefficient analysis.

Fluorescence recovery after photobleaching (FRAP). Maturation of droplets were processed on glasses after sealing. Droplets were bleached with 1% (Cy5) or 10% (Cy3, Fluorescein, EGFP) of laser power for 1 sec interactive bleaching using a 640 nm (Cy5), 561 nm (Cy3), or 488 nm (Fluorescein, EGFP) laser line. The droplets with >5 μm diameters were selected, and bleached regions were 1~2 μm diameters. Time-lapse images were collected in every 10 sec. Region of interest (ROI) was firstly set with the size of bleached region. At each time point, mean intensities of bleached region (I_R), neighboring unbleached region (I_U), and background region (I_B) with same ROI were measured. Recovered intensity ratio (I_t) were calculated by ($[I_R - I_B] / [I_U - I_B]$) at each time point, and fit to single exponential model ($I_t = I_\infty + (I_0 - I_\infty)e^{-kt}$) using Excel® (Microsoft® 2016), where I_0 is the ratio at the start of bleaching, I_∞ the ultimate recovery, and k the exponential constant. The mobile fraction of each

curve was calculated by ([I_B - I_0] / [I_∞ - I_0]), where I_B is the initial ratio before bleaching. Half-times were calculated by (ln2/k). 15 droplets from at least 3 independent experiments were selected for the analysis of all diffusions.

Droplet-droplet & Droplet-free tetramer interaction analysis. The maturation of pre-made droplets was processed in 1.5 mL Eppendorf tubes. 5 min or 60 min maturated droplets were mixed with a 10 μL : 10 μL volume ratio (FUS & TAF) or 12 μL (LAF) : 9 μL (FUS or TAF) ratio to equalize final concentrations of mixed scaffolds. Solutions were maintained for 5 min, and 5 μL of solution with droplets were observed on glasses. To generate free LAF tetramer solution without droplets, the maturated droplet solution was centrifuged at 20000 g at 25 °C for 10 min, and the supernatant was isolated.

Surface tension comparison. Surface tensions of droplets were determined by measuring contact angle values of various IDR droplets on glass surfaces. IDR droplets were formed with 2 μM fluorescein-tagged scaffolds, and placed on silanized hydrophobic or bare glass surfaces 5 min after phase separation. Droplet Z-stack images were collected by the LSM 780 laser scanning confocal microscope (Carl Zeiss, LSM780). Orthogonal images of droplets were analyzed to determine contact angles by ImageJ (NIH).